Experimental And Numerical Modeling Of The Flow Field In An Industrial Bronze Caster – Improving The Numerical Model

S. Eck[1], C. Pfeiler[1], A. Kharicha[1], A. Ludwig[1] and J. W. Evans[2]

[1]Dept. Metallurgy, University of Leoben, A-8700 Leoben, Austria
[2]Chair for Mineral Engineering, Mat. Sci. & Eng. Dept. University of California, Berkeley, CA-94720, USA

Keywords: Bronze casting, numerical model, water model

Abstract

In previous work the influence of the casting speed on the flow field and the shape of the solidification front in an industrial 0.82 x 0.25 x 0.8 m³ bronze caster had been investigated. Both numerical and experimental model represented 1:1 the real caster geometry. A comparison of the results of both numerical and experimental models for the flow during the casting process showed a good agreement in the qualitative velocity fields (flow direction and vortex formation). This work represents a parameter study of the numerical model with variations of the turbulence conditions at the inlet in order to clarify their influence on the flow field in the caster. In order to find the best boundary condition at the inlet, the numerical calculations for water have been compared with the measured flow fields in the water model. The new boundary conditions were then applied to the numerical model of the bronze casting process.

Introduction

In the casting of real metals the opacity of the melt and the high temperatures involved make it difficult to measure, or even observe, the flow patterns resulting from different metal delivery devices. Consequently, mathematical and physical modeling have been extensively used to determine the flows in casters, particularly those of steel casters. While mathematical models have been widely accepted, their performance has frequently been judged by their ability to predict flows measured in physical (water) models [1-5]. Physical modeling of the flow fields in the liquid melt is often performed by using water models and Particle Image Velocimetry (PIV) or similar flow field measurement techniques.
For non-ferrous metals with high thermal conductivity such as Al and Cu alloys the solidification front is close to the entry nozzle and this has therefore to be taken into account in both numerical and experimental modeling of the casting process. Xu et al. [6] have shown that in the case of Al direct chill casting the distance between entry of the liquid metal and the solidification front is in the order of 0.4 m. Recent calculations and cooperation with industrial partners revealed that in the case of Cu based alloys this distance is of the same order of magnitude [7-9]. Therefore, if a physical model of the flow fields appearing in these casting processes is to be realistic, it has to include the distance and shape of the solidification front. In real casting the shape of the solidification front depends on the casting material constants like thermal conductivity, viscosity, and density as well as on the casting parameters such as casting speed, cooling geometry and cooling efficiency.

In previous publications the authors showed how the flow in a real industrial bronze caster had been modeled by a water model [1, 2]. A PIV setup had been built and the flow fields have been measured along the wide symmetry plane. Those flow fields were time averaged by statistics on up to 500 instantaneous PIV measurements and it was shown that those time averaged PIV

results were comparable to steady state CFD calculations for water [1]. An experimentally determined solidification front shape had been delivered by a bronze manufacturing industry partner for a given casting velocity and this shape had been modeled by a flexible "solidification front module" in the water model [1]. Next, numerical simulations of the bronze caster had been performed with CFD to show the influence of the casting speed on the shape of the solidification front. The solidification front module of the water model was adapted according to the computed shapes and the resulting flow fields of the water model were compared with the numerical predictions for bronze [2].

When comparing the flow in liquid metal and in water and based on the simplifications of isothermal flow, the Reynolds number $\mathrm{Re} = u\,L\,/\,\nu$ has to be constant, where u is the mean fluid velocity, L is the characteristic length and ν is the kinematic fluid viscosity. For the modeled casting process, the casting speed determined the flow rate Q, e.g. for 1 mm/s casting speed the flow rate was $Q = 0.82$ m x 0.25 m x 0.001 m/s = 2.05 x 10^{-4} m³/s. The velocity at the inlet of the water model is then linked to the flow rate by the area of the inlet. For the 1:1 model, the characteristic lengths were constant, thus the water velocity (and the flow rate) were scaled by the ratio of the kinematic viscosities of liquid bronze and water to keep the Reynolds numbers constant. A comparison of the results of both numerical and experimental models for the flow during the casting process showed a good agreement in the qualitative velocity fields; i.e. both models showed the same flow directions and the same development and position of vortices in the flow field. However, discrepancies were observed in the quantitative comparison of the velocity profiles along defined vertical lines, i.e. the measured inlet jet was wider and had a higher maximum velocity then the measured jet in the water model. To calculate the flow fields and the shape of the solidification front, the commercial CFD package FLUENT [10] had been used. To calculate the solidification front shape, FLUENTs integrated solidification module [10] had been applied. The observed discrepancies in the line profiles indicated that the turbulence model had to be improved. The presence of the well-known "round jet anomaly" at the nozzle requires the use of a proper turbulence model. In contrast to the standard k-ε, the realizable k-ε turbulence model [11] is known to correctly predict the spreading rate of a round jet. The realizable k-ε is intended to correct the round jet deficiency by defining the variable C_μ and by applying a new equation for the turbulent dissipation [11]. In the case of a cylindrical inlet with a known diameter (in this case 26 mm) the implementation of the realizable k-ε model in FLUENT allows the user to define the turbulence intensity with a single variable as inlet boundary condition [10]. Thus the aims of the work presented here were to

a) estimate the influence of the turbulence intensity as boundary condition at the inlet on the jet velocity and the jet dimension for the water model,
b) compare the numerical results for various turbulence intensity conditions with the values measured by PIV in the water model to find the best values,
c) apply the new boundary conditions to the calculation of the bronze direct chill casting process and estimate the effect of the jet dimensions and velocities on the shape of the solidification front.

Simulation Model Description

In this section the numerical model for predicting solidification within a turbulent flow field in a bronze continuous caster is presented. FLUENT [10] was used to perform the simulations.
The energy conservation equation of the enthalpy-formulation is

$$\rho\frac{\partial h}{\partial t} + \rho\nabla\cdot\left(\vec{u}h\right) = \nabla\cdot\left(k_{eff}\nabla T\right) - Q_L\,, \qquad (1)$$

where, h is the sensitive enthalpy defined as

$$h = h_{ref} + \int_{T_{ref}}^{T} c_p \, dT \,. \tag{2}$$

h_{ref} is the reference enthalpy at the reference temperature T_{ref} and c_p is the specific heat. ρ is the density of the melt, $\vec{u}$ the velocity and k_{eff} is the effective conductivity which is defined as $k_{eff} = k + k_t$. Here, k defines the thermal conductivity of the material and k_t is the turbulent thermal conductivity.
The source term Q_L concerning the latent heat in a single phase solidification model can be written as

$$Q_L = \rho L \frac{\partial f_l}{\partial t} + \rho L \nabla (\vec{u} \cdot f_l). \tag{3}$$

Two terms have to be considered to treat the latent heat, the explicit latent heat term, $\rho L \partial f_l / \partial t$ and the convective term, $\rho L \nabla (\vec{u} \cdot f_l)$. The relationship between liquid fraction f_l and the temperature was assumed to be linear. The latent heat, L, is released in the mushy zone. In continuous casting the solidifying shell is moving downwards with a constant casting velocity $\vec{u}_{pull}$. The melt which is being solidified has the speed of the solidifying shell.
The mass and momentum conservation equations are given by

$$\nabla \cdot \vec{u} = 0 \,, \tag{4}$$

$$\rho \frac{\partial \vec{u}}{\partial t} + \rho \nabla \cdot (\vec{u} \otimes \vec{u}) = -\nabla p + \nabla \left(\mu_{eff} \nabla \cdot \vec{u} \right) + \vec{S}_D \,, \tag{5}$$

where $\mu_{eff} = \mu_l + \mu_t$ is the effective viscosity due to turbulence, for which the realizable k-ε model is used. μ_l is the dynamic viscosity, μ_t, is the turbulent viscosity, which is defined by $\mu_t = \rho C_\mu k^2/\varepsilon$ and p is the static pressure. The realizable k-ε is intended to correct for the "round jet" deficiency of the standard k-ε model by defining the variable C_μ and with the a new equation for the turbulent dissipation ε. The turbulent intensity is defined as the ratio between the typical turbulent velocity fluctuation over the mean velocity magnitude ($2k^{0.5}/3U$) [11].
The pressure drop caused by the presence of solid material is considered as a momentum sink, $\vec{S}_D$, in the momentum conservation equation. The mushy zone is treated as a permeable medium with a permeability according to the Blake-Kozeny law. The momentum sink for bronze, was taken correspondingly from [10]:

$$\vec{S}_D = -\frac{(1 - f_l)^2}{f_l^3} A_{mush} \left(\vec{u} - \vec{u}_{pull} \right). \tag{6}$$

Here, A_{mush} depends on the primary dendrite arm spacing of the solidified bronze [7] and the melt viscosity. This corresponds to a value for $A_{mush} = 10^8$. Corresponding sink terms were also added to all of the turbulence equations in the mush and solidified areas.

Simulation Parameters

Preceding studies demonstrated a symmetric and stable flow field in the modeled bronze caster [2]. Utilizing the double symmetry, the calculation domain (Figure 1) consisted of a quarter of the 0.66 m long upper part of the caster including a cylindrical submerged entry nozzle (SEN) with two nozzle ports. The computational domain was discretized into structured hexahedral volume elements in the mould and into unstructured polyhedral volume elements in the

submerged entry nozzle. The whole grid consisted of ~ 280,000 cells in the mold and ~8,500 cells in the nozzle. Two different geometries (CASES) were used for the simulations. In CASE1 the nozzle flow was neglected as was the case in preceding studies [1, 2]. Here, the inlet was positioned at the nozzle ports of the SEN. In CASE2 the nozzle flow was included in the calculation, i.e. the inlet was positioned at the top surface of the nozzle.

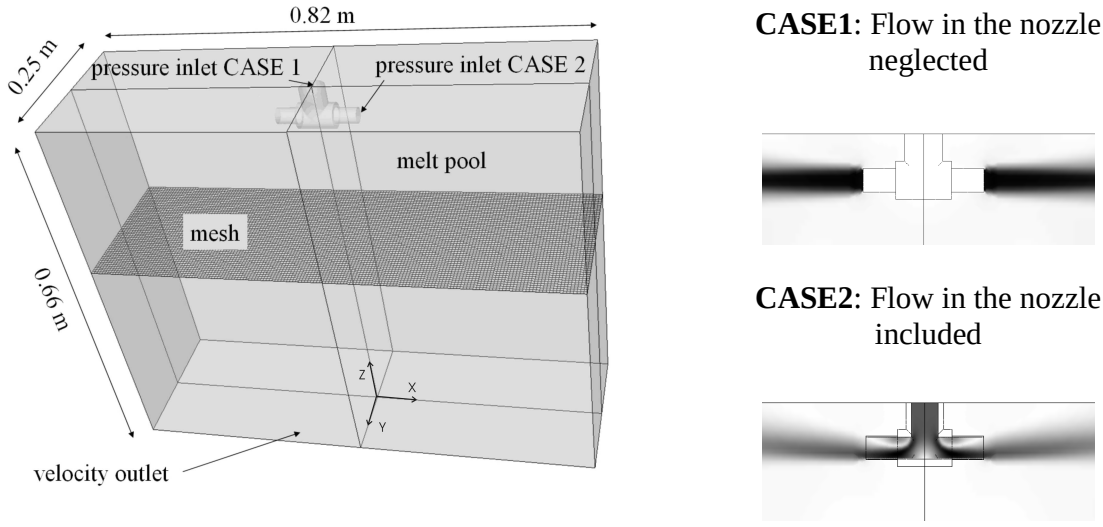

Figure 1: Geometry of the simulation domains for CASE1 and CASE2.

In both cases the inlet was defined as a pressure inlet. The mass flow rate was therefore defined by the boundary condition at the bottom of the domain where a constant downwards velocity, related to the bronze casting speed, was applied. The top surface of the liquid melt pool being in contact with the casting slag was presumed to be flat and a free-slip condition was used. Two different fluids, water and bronze, were used in the presented simulations. The applied material properties and process parameters for both fluids are shown in Table 1.

Table 1: Material properties and process parameters used for the presented calculations

Water Simulations			**Bronze Simulations**		
Density	998.2	[kg/m³]	Density	7810	[kg/m³]
Viscosity	1.003E-3	[kg/(m s)]	Viscosity	32E-3	[kg/(m s)]
Outlet velocity	1.85E-3	[m/s]	Outlet velocity (= Casting Speed)	8.50E-4	[m/s]
Turbulence intensity at the inlet	1-50	[%]	Turbulence intensity at the inlet	3-5	[%]
			Specific heat	454	[J/(kg K)]
			Thermal conductivity	92	[W/(m K)]
			Casting temperature	1390	[K]
			Heat transfer coefficient	3000	[W/(m²K)]
			Free stream temperature	500	[K]
Both water and bronze calculations					
Domain width	0.82	[m]	Turbulence length scale	0.026	[m]
Domain thickness	0.25	[m]	Reynolds number at the inlet	21700	[-]
Domain length	0.66	[m]			

For the computation of the bronze casting a constant heat transfer coefficient for the narrow and the wide face of the mould was used. Its value had been adjusted until the calculated sump depth for a given casting speed corresponded to the sump depth supplied by the industry partner [7].

Results And Discussion

Water Model

In the following section the predictions of the flow field in the water model as results of the various calculations will be compared both qualitatively (flow direction) and quantitatively (flow velocity). Figure 2 shows the qualitative comparison of the flow fields predicted for isothermal flow of water with the inlet conditions of CASE1 on the left, and CASE 2 in the center. In both cases the turbulence intensity at the inlet was set to 5%. The results of the time averaged PIV measurements in the water model are shown in Figure 2 on the right. The details of the PIV measurements were given in ref. [1, 2]. The flow field of CASE1 with a horizontal inlet shows a jet that is basically horizontal with a slight upwards component. This upwards component is driven by a vortex that in turn is created by the downwards flow where the incoming jet hits the wall and the resulting upwards flow in the center. The results of CASE2 show a vertical flow in the nozzle that reflects from the lower horizontal part of the nozzle and therefore shows a jet direction that is tilted upwards in the main domain. This upwards tilt of the jet was also observed in the time averaged PIV measurements of the water model which indicates that CASE 2 is a better model to predict the jet position.

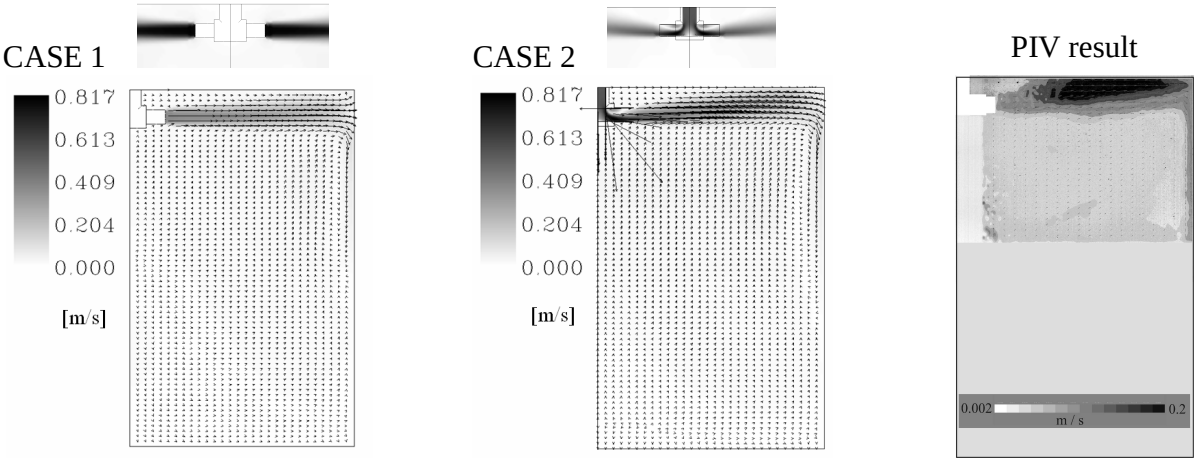

Figure 2: Comparison of the flow field directions. Left: calculated for CASE1; center: calculated for CASE2; right: measured with time averaged PIV. The corresponding grey scales show the velocity magnitude [m/s].

For a quantitative comparison of the results of the different calculations vertical lines were defined in the wide symmetry plane at 0.205 m distance from the nozzle center, i.e. along z at x = 205 and y = 0. To compensate the fact that the PIV results represent the velocities in a 10 mm wide illumination plane [1, 2], further lines were defined 5 mm in front of the center plane, i.e. along z at x = 205 mm and y = 5 mm. The position of the center plane “quarter lines” in the computational domain is sketched in Figure 3. The velocity magnitude was exported and plotted versus the z-position, i.e. the distance from the top surface of the liquid domain. A representative plot of a velocity line profile is shown on the right side of Figure 3. The shape of the jet velocity was found to be very close to a slightly asymmetric Gaussian. Therefore, the values for the

maximum velocity in the jet and the full width at half maximum (FWHM) of the jet were taken from Gauss fits instead of measuring them “by hand”.

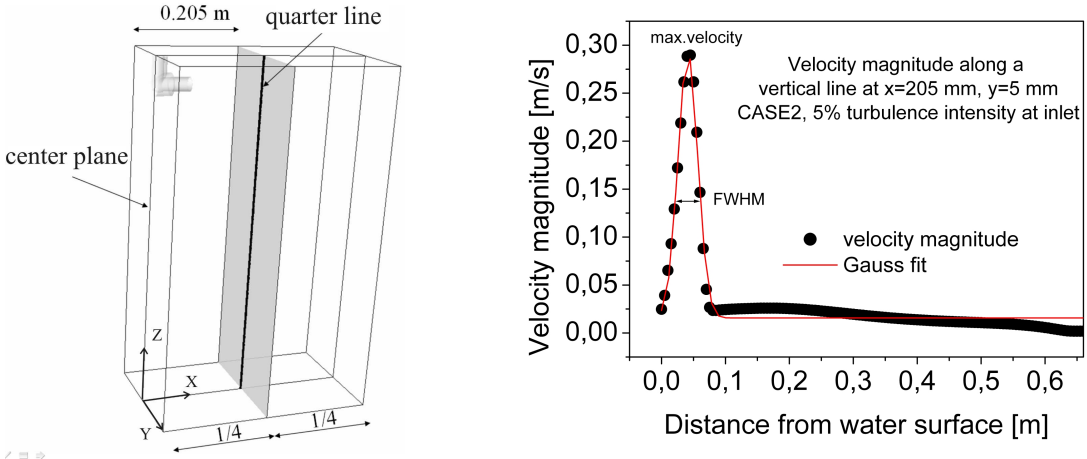

Figure 3: Position of the vertical lines taken for the quantitative comparison of the flow fields and a sample of a Gaussian fit of the jet velocity profile at this position.

Figure 4 shows the results of the parameter study for the turbulence intensity at the inlet at different positions in the water model and for the 2 different inlet geometries CASE1 and CASE2. In Figure 4a the maximum velocity in the jet was plotted versus the turbulence intensity, in Figure 4b the width of the jet was plotted versus the turbulence intensity. The plots show that for CASE1 the value of the turbulence intensity that had been set at the horizontal inlet strongly influenced the maximum velocity in the jet as well as the width of the jet. A higher turbulence intensity at the horizontal inlet resulted in a wider jet with a lower maximum velocity. This is in agreement with the general understanding of turbulence as with higher turbulence more kinetic energy (i.e. velocity) is spent on the formation of eddies which in turn results in a wider jet.

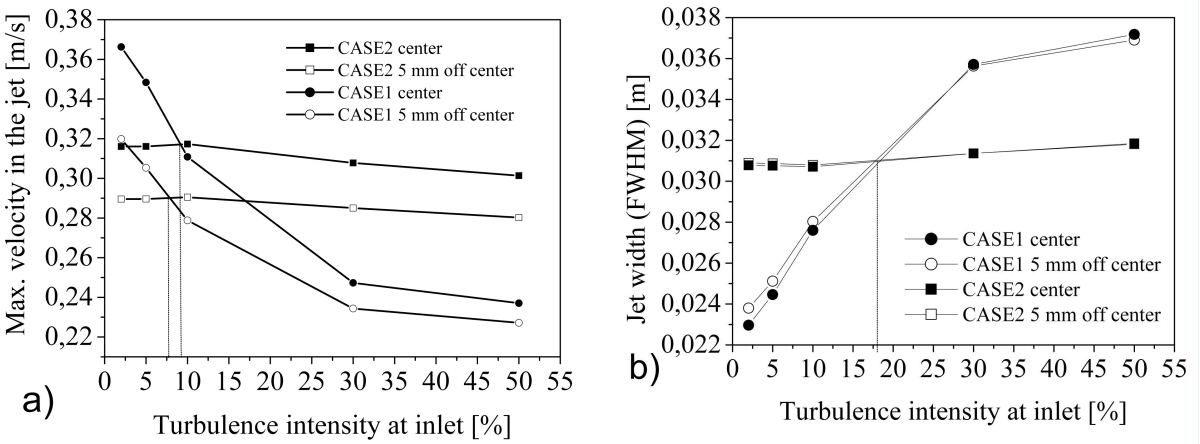

Figure 4: Results of the parameter study for the turbulence intensity at the inlet at different positions in the water model and for the 2 different inlet geometries CASE1 and CASE2;
a) maximum velocity in the jet versus the turbulence intensity, b) width of the jet versus the turbulence intensity.

A comparison of the lines at y = 0 (center plane) and y = 5 mm showed that the maximum velocity in both CASE1 and CASE2 decreased with increasing distance from the center plane. This can be understood by the fact that the 3 dimensional shape of the jet is a cone with the maximum velocity in the center and gradually decreasing velocity with increasing distance from

its center line. In consideration of this fact and the fact that the time averaged PIV result also represent a space averaged velocity field due to the 10 mm wide illumination plane, a quantitative comparison has to be done very carefully. PIV experiments for the same flow rate as presented in this study resulted in a jet with a maximum velocity of 0.21 ± 0.01 m/s and a FWHM of 0.040 ±0.001 m (results not shown). PIV measurements with various flow rates from 2.5×10^{-4} m³/s to 5×10^{-4} m³/s (4 to 8 GPM) showed that the maximum velocity in the jet scaled exactly with the flow rate and that the FWHM of the jet linearly increased from 34 to 37 mm with increasing flow rate (results not shown). If one would only consider the parameter study for CASE1 this would indicate that a (very unrealistic) turbulence value of more than 50% at the horizontal inlet represents the measured flow best. However, this would not clarify the origin of that high turbulence intensity. The parameter study for CASE2 clearly indicates that the change of the turbulence intensity of the top of the nozzle has only a minor effect on the jet velocity and the jet shape. Thus the turbulence is generated within the nozzle, presumably where the inlet flow hits the nozzle bottom. A direct comparison of the lines for CASE1 and CASE2 in Figure 4a show intersection of the curves at ~7 and ~9% turbulence intensity, i.e. an average turbulence intensity of ~ 8% in CASE1 resulted in the same maximum velocity as in CASE2. Regarding the width of the jet in Figure 4b, the intersection of the center lines for both geometries was at ~18% turbulence intensity. As a consequence of the geometry study it can be concluded that the discrepancy between the measured and the calculated velocity and shape of the jet could be partially (but not fully) eliminated by setting the turbulence intensity at the inlet to a higher value. According to the geometry study the turbulence intensity at the horizontal inlet should be set to a value between 8% and 18% if the flow through the nozzle is not calculated. The actual value depends on whether the correct prediction of the velocity or the width of the jet is considered more important.

Bronze Caster Solidification Model

As a consequence of the geometry study, new calculations of the bronze casting process have been performed to clarify the influence of the jet position and shape on the shape of the solidification front hat had been calculated and modeled in previously published work [1, 2]. To compare the results of the calculations for the two different geometries, the solidification front in the center plane was defined as the line where the liquid fraction f_l had a value of 99%. Figure 5 shows a plot of the solidification front lines in the center plane for CASE1 and CASE2. Despite the fact that the different inlet geometries showed a clear influence on the jet, the solidification front shapes only showed minor differences.

Conclusions

Calculations of the water flow showed that for the given nozzle geometry of an inverted T the flow through the nozzle has to be included in the calculation to correctly predict the jet position in the caster. The observed discrepancy between the measured and the calculated velocity and shape of the jet [2] could be partially (but not fully) eliminated by setting the turbulence intensity at the inlet to a higher value. According to the geometry study the turbulence intensity at the horizontal inlet should be set to a value between 10 and 20 if the flow through the nozzle is not calculated.

Calculations of the bronze casting process showed that for a simple prediction of the solidification front shape in the caster the flow in the nozzle itself may play a minor role. However it is obvious from the results that the turbulence settings at the inlet have a strong influence on the jet. For more sophisticated predictions of the casting process such as macro segregation during the casting process this has to be taken into account.

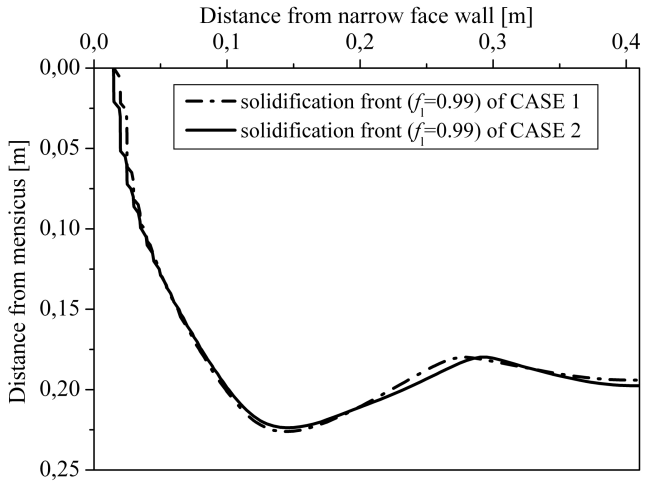

Figure 5: Calculated solidification front (defined as f_l = 0.99) plotted as lines in the center plane for the two different inlet geometries CASE1 and CASE2.

References

1. S. Eck, A. Ludwig, D. Mazumdar and J.W. Evans, *Proc. 5th Dec. Conf. Solidification Processing*, Sheffield, (July 2007**)**, 483-487.

2. S. Eck, C. Pfeiler, F. Mayer, A. Ludwig and J. W. Evans, *Int. J. Cast Metals Research*, (2008), in press.

3. J.W. Evans, "*Computational fluid dynamics in Mineral & Metals Processing and Power Generation*", CSIRO, Clayton, Victoria, Australia, (1997), 7-20.

4. H. Bai and B.G. Thomas, *Metall. Mater. Trans. B*, 32B (2) (2001), 253-267.

5. Brian G. Thomas, Quan Yuan, S. Sivaramakrishnan, and S.P. Vanka, *JOM-e*, Vol. 54, No. 1, (2002), e-journal.

6. D. Xu, W. Kinzy Jones and J.W. Evans, *Metall. Mater. Trans. B*, vol 29B, (1998), 1281.

7. Private communication with researchers at the bronze manufacturer Wieland-Werke AG, Graf Arco-Str. 36, 89079 Ulm, Germany, (2006).

8. Ludwig, et. al, *Mat. Sci. Eng. A*, 413-414, (2005), 485-489.

9. M. Gruber-Pretzler, et. al., "*Continuous Casting*", (2006); Ed. H. R. Müller, Germany, Wiley-VCH, ISBN-13: 987-52731341-9, 219-225 .

10. FLUENT 6.0 user's guide, FLUENT Inc., Lebanon, NH, USA

11. T.-H. Shih, W.W. Liou, A. Shabbir, and J. Zhu, *Computers Fluids*, 24(3), (1995), 227-238.